

Effect of particle statistics in strongly correlated two-dimensional Hubbard models

Ehsan Khatami and Marcos Rigol

*Department of Physics, Georgetown University, Washington District of Columbia, 20057, USA and
Physics Department, The Pennsylvania State University,
104 Davey Laboratory, University Park, Pennsylvania 16802, USA*

We study the onset of particle statistics effects as the temperature is lowered in strongly correlated two-dimensional Hubbard models. We utilize numerical linked-cluster expansions and focus on the properties of interacting lattice fermions and two-component hard-core bosons. In the weak-coupling regime, where the ground state of the bosonic system is a superfluid, the thermodynamic properties of the two systems at half filling exhibit very large differences even at high temperatures. In the strong-coupling regime, where the low-temperature behavior is governed by a Mott insulator for either particle statistics, the agreement between the thermodynamic properties of both systems extends to regions where the antiferromagnetic (iso)spin correlations are exponentially large. We analyze how particle statistics affects adiabatic cooling in those systems.

PACS numbers: 67.85.-d, 05.30.Jp, 05.30.Fk, 05.70.-a

I. INTRODUCTION

The Fermi-Hubbard model has been the *de facto* playground for exploring the properties of high-temperature superconductors for more than two decades [1]. Yet, still no analytical solution exists in more than one dimension, and state-of-the-art numerical calculations prove very difficult in regimes where the average number of fermions per site is different from 1. Unveiling the properties of the model in the latter regime, and addressing whether it supports superconductivity, may be crucial in understanding high-temperature superconductivity [2].

More than a decade ago, it was proposed that one could “solve” strongly-interacting quantum lattice models by “simulating” them using ultracold atoms in optical lattices [3]. More recently, the Mott insulator in the Bose-[4] and the Fermi-Hubbard [5] models were realized in these experiments. However, current accessible temperatures for fermions are still higher than one needs to observe even the relatively high temperature antiferromagnetic Néel transition in three dimensions.

These experiments are done using atoms with internal degrees of freedom, which can be selected to emulate not only two-specie fermions (Fermi-Hubbard model) and single-specie bosons (Bose-Hubbard model), but also particles with exotic statistics and/or pseudo-spins [6–10]. For instance, it has been shown that experiments with two-component (spin-1/2) bosons can lead to the realization of quantum spin models with tunable parameters [11–15]. In the specific case where the intra-specie onsite repulsion is infinite, multiple occupancy of a single specie per site is forbidden. This case realizes an effective two-component hard-core boson (2HCB) model, which could be thought of as the bosonic equivalent of the Fermi-Hubbard model [11, 16, 17]. Similar to fermions, in the strong-coupling regime (large inter-species interactions), the low-energy properties of this model can be described by a t - J model [18, 19].

Despite the outward similarities between the Fermi-Hubbard model and the 2HCB-Hubbard model (in one

dimension they share identical thermodynamic properties) in two dimensions, particle statistics plays a fundamental role in the properties of the system as the temperature is lowered, and in the selection of the ground state. At half filling, the ground state of fermions in two spatial dimensions is a Mott insulator with a long-range Néel order for any value of the interaction strength, U . For 2HCBs, there is a quantum critical point at interaction $U_c/t \sim 11$, where t is the hopping amplitude, which separates a phase with two miscible strongly-interacting superfluids (2SF) at small inter-specie interactions from a Mott insulator super-counter-fluid (SCF) [13] phase in the strong-coupling regime [16]. The latter state corresponds to a superfluid of pairs of bosons from one specie and holes of the other specie, and can also be interpreted as a long-range XY -ferromagnet in the iso-spin language. It is expected that such big contrasts in the nature of the ground states result in significant differences in the thermodynamic properties as well. Hence, for validating experiments with ultracold gases, which are performed at finite temperature, it is important to have access to exact quantitative results for the finite-temperature properties of the two systems.

While there have been numerous finite-temperature numerical studies of fermions in optical lattices [20, 21], the same is not true for 2HCBs, in particular in two dimensions. In one dimension, calculations were done introducing a generalized Jordan-Wigner transformation [22]. The three-dimensional model with *attractive* interaction was studied to describe the supersolid state of ^4He [23, 24]. Recently, dynamical mean-field theory results have been reported for the two-component (soft-core) Bose-Hubbard model in two dimensions with an average of 1/2 particle of each specie per site and large intra-specie interactions [15, 25]. It was found in those studies that, upon heating from zero temperature, the system quickly enters an unordered Mott insulator. These findings have been complemented by finite-temperature quantum Monte Carlo (QMC) simulations of magnetic phases [17, 26] as well as a field-theoretical

treatment [27] in the hard-core limit.

Here, we utilize numerical linked cluster expansions (NLCEs) to provide a comparative analysis between finite-temperature properties, such as the equation of state, entropy, specific heat, double occupancy, and spin correlations, of fermions and 2HCBs. We are particularly interested in identifying at what temperatures particle statistics become important in different interaction regimes, as well as what kind of qualitatively different behavior is produced by the statistics of the particles below those temperatures. We also discuss the implications of having bosonic vs fermionic statistics for adiabatic cooling protocols and for detecting short-range spin correlations in ultracold atoms experiments. We note that the lowest temperatures that are accessible with NLCEs are typically higher than the crossover temperatures to the XY -ferromagnet phase [15]. Therefore, the behavior of the strongly-correlated systems that we study at half filling is that of a Mott insulator with large spin correlations for either particle statistics.

We show that, in the weak-coupling regime ($U < U_c$), where the bosonic system has a superfluid ground state, the disagreement between properties of fermions and 2HCBs is apparent at relatively high temperatures (of the order of the hopping). In contrast, by increasing U in the strong-coupling regime, the agreement between the thermodynamic properties of the two systems extends to lower temperatures. For 2HCBs, although the z -antiferromagnetic Néel ground state is known to win over the XY -ferromagnet only in cases where the two species have different hopping amplitudes, the two phases are very close in energy for equal hopping amplitudes (the case considered here) as only terms beyond the second order perturbation in interaction determine the difference [11, 13]. Consistent with this picture, we find that at strong interactions, short-range z -antiferromagnetic correlations are large in the low-temperature Mott region and very close for the two particle statistics. Given that there are more efficient cooling techniques for bosons than for fermions, one could envision probing finite-temperature fermionic correlations using strongly correlated bosonic systems. Here, we present evidence that, through an adiabatic cooling mechanism that takes place in the bosonic system, the region with exponentially large antiferromagnetic (AF) correlations in two dimensions is more easily accessible with 2HCBs than with fermions.

The exposition is organized as follows: In Sec. II, we introduce the model and discuss the NLCEs used in this study. We present the results for the thermodynamic properties of the models as well as their implications for the optical lattice experiment in Sec. III. Our findings are summarized in Sec. IV.

II. THE MODEL AND NLCEs

We consider the two-dimensional (2D) Hubbard Hamiltonian on the square lattice:

$$\hat{H} = -t \sum_{\langle i,j \rangle \sigma} (\hat{a}_{i\sigma}^\dagger \hat{a}_{j\sigma} + \text{H.c.}) + U \sum_i \hat{n}_{i\uparrow} \hat{n}_{i\downarrow} - \mu \sum_i (\hat{n}_{i\uparrow} + \hat{n}_{i\downarrow}) \quad (1)$$

where $\hat{a}_{i\sigma}^\dagger$ ($\hat{a}_{i\sigma}$) creates (annihilates) a particle with spin σ (for simplicity, we use spin instead of isospin for bosons too) on site i , and $\hat{n}_{i\sigma} = \hat{a}_{i\sigma}^\dagger \hat{a}_{i\sigma}$ is the number operator. $\langle \dots \rangle$ denotes nearest neighbors (NN), and U (> 0) is the strength of the onsite repulsion. $t = 1$ ($\hbar = 1$ and $k_B = 1$) sets the unit of energy throughout this paper. We consider two different particle statistics: fermions ($\hat{a}_{i\sigma} = \hat{f}_{i\sigma}$) and 2HCBs ($\hat{a}_{i\sigma} = \hat{b}_{i\sigma}$). The 2HCB operators satisfy the following commutation relations and constraints:

$$[\hat{b}_{i\sigma}, \hat{b}_{j\sigma'}^\dagger] = \delta_{ij} \delta_{\sigma\sigma'}, \quad \hat{b}_{i\sigma}^{\dagger 2} = \hat{b}_{i\sigma}^2 = 0. \quad (2)$$

Numerical linked-cluster expansions

We solve the Hamiltonian (1) using the NLCEs introduced in Ref. [28]. In NLCEs, an extended property of the lattice model per site in the thermodynamic limit, P , is expanded in terms of contributions from all of the clusters, up to a certain size, that can be embedded in the lattice:

$$P = \sum_c L(c) w_p(c), \quad (3)$$

where c represents the clusters. The contribution of each cluster with a particular topology is proportional to the number of ways it can be embedded in the lattice per site, $L(c)$, and its weight for the property of interest, $w_p(c)$. The weights are computed based on the inclusion-exclusion principle and given the property for each cluster, $\mathcal{P}(c)$, which is calculated using exact diagonalization [28]:

$$w_p(c) = \mathcal{P}(c) - \sum_{s \subset c} w_p(s). \quad (4)$$

Here, we carry out the calculations up to the ninth order in the site expansion (maximum cluster size of nine sites).

NLCEs do not suffer from statistical or systematic errors, such as finite size effects and are not restricted to small or intermediate interaction strengths. For this reason, they are complementary to more commonly used methods, such as QMC simulations and dynamical mean-field theory, especially in the strong-coupling regime ($U \gg t$) where computations in the latter approaches become more challenging. However, NLCE results are useful only in the temperature region in which the series converge, which has been shown to extend beyond the region

accessible within high-temperature expansions [28, 29]. The convergence of NLCEs can be accelerated by means of numerical resummations algorithms [28]. Here, we use Euler and Wynn methods with different parameters and plot the resulting last two orders (or only the last order when the two are indistinguishable in the figures). The results from all of those algorithms agree with each other in the regions shown within the small fluctuations seen in some cases at the lowest temperatures. These fluctuations, which occur below the convergence temperature of NLCE direct sums, arise from numerical instabilities in the resummations routines.

We work in the grand canonical ensemble [29], and so, the exact diagonalization for every finite cluster in the series is performed in all particle and spin sectors. For each U , the partition function and all other observables are calculated in a dense grid of chemical potentials (μ) and temperatures (T). This allows us to study their behavior at constant density $n = \langle \hat{n}_\uparrow + \hat{n}_\downarrow \rangle = 2\langle \hat{n}_\sigma \rangle$ [29], where $\langle \dots \rangle$ denotes the expectation value. Since only NN hopping is considered, properties of the particle-doped system can be expressed in terms of those for the hole-doped system. Hence, in most cases away from half filling, we show results only for the hole-doped system ($n < 1$).

III. RESULTS

Entropy and specific heat

Generally, when using QMC-based methods, the specific heat (C_v) or the entropy (S) calculations involve numerical derivatives and/or integration by parts [30, 31], which can introduce systematic errors. Within NLCEs, these two quantities are computed directly from their definitions:

$$S = \ln(Z) + \frac{\langle \hat{H} \rangle - \mu \langle \hat{n} \rangle}{T}, \quad (5)$$

where Z is the partition function, and

$$C_v = \left(\frac{\partial \langle \hat{H} \rangle}{\partial T} \right)_n = \left(\frac{\partial \langle \hat{H} \rangle}{\partial T} \right)_\mu + \left(\frac{\partial \langle \hat{H} \rangle}{\partial \mu} \right)_T \left(\frac{\partial \mu}{\partial T} \right)_n. \quad (6)$$

Since we work in the grand canonical ensemble, where the chemical potential and not the density is the control parameter, we have written this expression in a more suitable form for numerical evaluation. After straightforward mathematical derivations, using Maxwell equations, one can obtain the following closed form for the specific heat in terms of expectation values that can be computed directly in NLCEs:

$$C_v = \frac{1}{T^2} \left[\langle \Delta \hat{H}^2 \rangle - \frac{(\langle \hat{H} \hat{n} \rangle - \langle \hat{H} \rangle \langle \hat{n} \rangle)^2}{\langle \Delta \hat{n}^2 \rangle} \right], \quad (7)$$

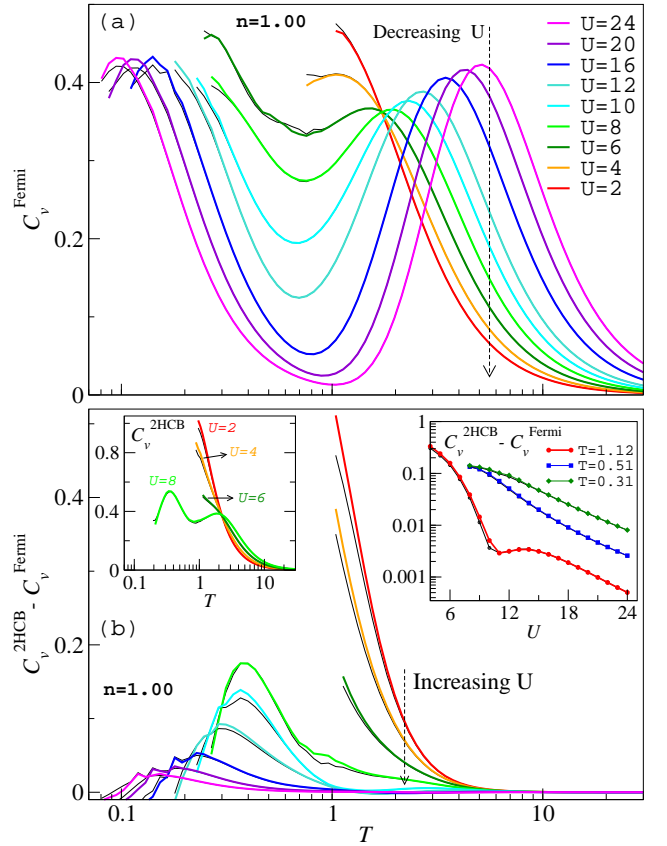


FIG. 1. (Color online) (a) Specific heat (C_v) of the Fermi-Hubbard model at half filling vs temperature for values of the onsite interaction ranging from $U = 2$ to three times the bandwidth ($U = 24$). (b) Difference between the specific heat of the Fermi-Hubbard model and the 2HCB-Hubbard model at half filling vs temperature, for the same interactions as in (a). The left inset in (b) shows C_v for the latter model vs T for $U = 2, 4, 6$ and 8 ; and the right inset shows the difference between C_v of the Fermi-Hubbard model and 2HCB-Hubbard model at half filling vs U at three different temperatures. We have used Euler sums for the last 6 terms. Thick (color) lines are the results of the sums up to the 9th order and thin (black) lines up to the 8th order.

where $\langle \Delta \hat{H}^2 \rangle = \langle \hat{H}^2 \rangle - \langle \hat{H} \rangle^2$, and similarly $\langle \Delta \hat{n}^2 \rangle = \langle \hat{n}^2 \rangle - \langle \hat{n} \rangle^2$.

We begin our study of the dependence of the observables on particle statistics as the temperature in the system is changed by showing, in Fig. 1, the specific heat for fermions and 2HCBs. Figure 1(a) shows the specific heat of the Fermi-Hubbard model from the weak-coupling regime to the strong-coupling regime with interactions up to three times the bandwidth ($U = 24$). The trend in the deviation of the specific heat for 2HCBs from that of fermions for different interaction strengths is depicted in Fig. 1(b), where we show the difference between the two. It is clear that for $U \lesssim 8$, the difference is significant at temperatures greater than 1. For example, as shown in the left inset in Fig. 1(b), the specific heat of 2HCBs for $U = 2$ is roughly twice as large as that of

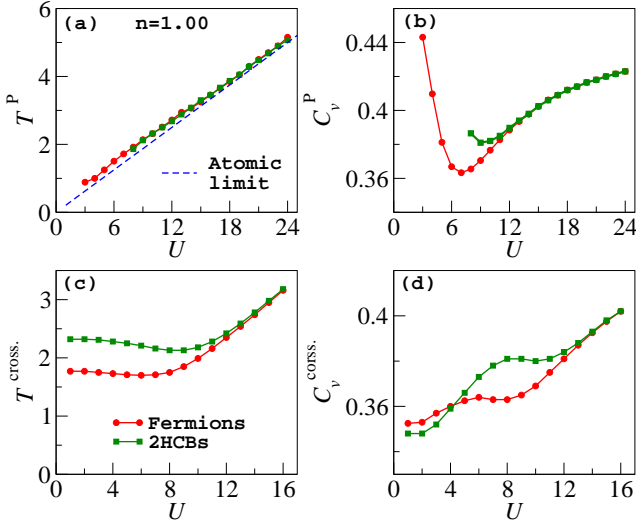


FIG. 2. (Color online) (a) Temperature and (b) value of the high-temperature peak of the specific heat (C_v^P) as functions of U . By decreasing U in the strong-coupling regime, C_v^P for the bosonic case deviates from the fermionic one around $U = 12$. For $U < 8$, the two peaks in the specific heat of 2HCBs merge, and the high-temperature peak is not well-defined anymore. (c) The location of the high-temperature crossing point between the specific heat curves for consecutive values of U . (d) The value of C_v at that crossing point.

fermions around $T = 1$. Although the exact trend of the former at lower temperatures cannot be resolved within our method, such large high-temperature values in comparison to those for the fermionic case are suggestive of the lack of a second peak at lower temperatures in the 2HCB model. This is also supported by a fast drop in the entropy (not shown). We have found that for $U = 2$, at $T \sim 0.8$, already $\sim 70\%$ of the infinite-temperature entropy has been quenched. For 2HCBs, a double-peak structure in the specific heat becomes apparent for $U \gtrsim 7$. At the same time, the minimum temperature at which NLCEs converge, which for smaller U is generally higher for 2HCBs in comparison to fermions, extends to roughly the location of the low-temperature peak.

For fermions, our NLCE calculations resolve the double-peak structure of the specific heat in the thermodynamic limit for $U \geq 6$. Since QMC simulations can access lower temperatures for $U \lesssim 6$, previous QMC studies of this model have established the existence of the low- T peak for any finite value of the interaction strength [32], which signifies the crossover to the phase with exponentially large AF correlations. In the strong-coupling regime, the specific heat results for fermions and 2HCBs are very close to each other at high temperatures ($T > 1$). In this regime, the difference between the C_v of the two particle statistics decreases systematically for all accessible temperatures as U is increased. As shown in the right inset in Fig. 1(b), the reduction of this difference is nearly exponential for large values of U .

The high- T peak, which is associated with the freez-

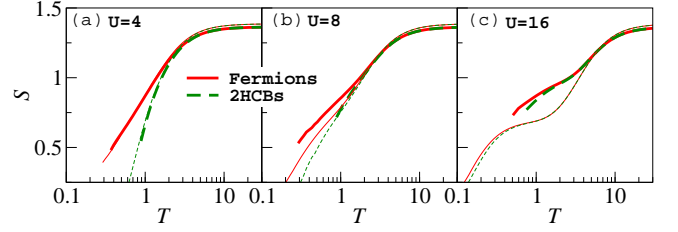


FIG. 3. (Color online) Comparison of the entropy vs temperature for $n = 0.85$ (thick lines) and $n = 1.00$ (thin lines) between the Fermi-Hubbard and the 2HCB-Hubbard models for (a) $U = 4$, (b) $U = 8$, and (c) $U = 16$.

ing of charge degrees of freedom and moment formation, moves to higher T as U increases. In the atomic limit ($t \rightarrow 0$), the location of the peak, T^P , is determined by $\alpha \tanh(\alpha) = 1$, where $\alpha = U/16T^P$, which can be approximated by $T^P = U/4.8$. For large U , and regardless of the particle statistics, we find a very good agreement with the atomic limit prediction for T^P [see Fig. 2(a)]. Note that there is no well-defined high- T peak in the specific heat of 2HCBs for $U < 7$. Unlike its position, the value of this peak does not change monotonically with increasing U and, as seen in Fig. 2(b), has a minimum around $U = 7$ for fermions and around $U = 9$ for 2HCBs. However, the relative change in the studied range of interactions is only about 20%. For large values of U , the area under the high- T peak of C_v/T also approaches $\ln(2)$, consistent with results in the atomic limit.

The low-temperature peak, which is associated with ordering of the moments, is expected to move to lower temperatures by increasing U . This is because, for large values of $U (\gtrsim 12)$, the low- T system is essentially described by the antiferromagnetic Heisenberg model with a characteristic energy scale of $J \propto t^2/U$ [21]. Therefore, the position of the low- T peak, which we do not report here, is expected to be inversely proportional to U .

An interesting feature discussed in the past for correlated fermionic systems is the near universal high- T crossing of the specific heat curves for different values of the interaction [32–34]. Due to its accuracy, NLCE provides an ideal tool for examining the precise behavior of the crossing point. We show its position, and the value of C_v at the crossing, in Figs. 2(c) and 2(d), respectively. We find that, for fermions, the temperature and the specific heat value of the crossing point between two consecutive values of U is nearly independent of U for $U \leq 8$ ($T^{\text{cross.}} \sim 1.75$, and $C_v^{\text{cross.}} \sim 0.36$), with changes of roughly 5%. These variations are slightly larger for 2HCBs in the same range of interactions.

Away from half filling, where the ground state of neither system is known, the trends in the deviation of finite-temperature properties of fermions and 2HCBs is different from the one reported so far. As an example, we show in Fig. 3 the entropy (for $U = 4, 8$, and 16) vs T for $n = 0.85$, and compare each curve with the one for $n = 1.00$. Interestingly, in the weak-coupling regime, the

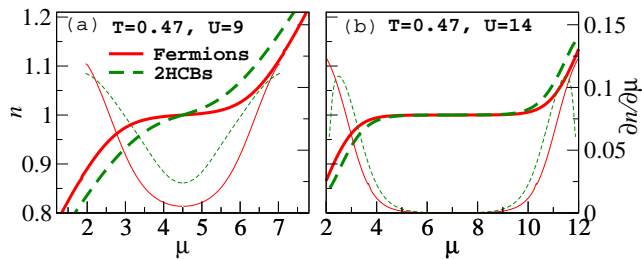


FIG. 4. (Color online) Equation of state and compressibility ($\partial n / \partial \mu$) vs μ of fermions and 2HCBs for (a) $U = 9$ and (b) $U = 14$ at $T = 0.47$. Thick lines show n and thin lines show the compressibility. At zero temperature, the density of fermions is pinned at unity for $|\mu| < \Delta$, where Δ is the charge gap, regardless of U . For bosons, the system has no gap for $U < U_c$. Here, Wynn resummations with three cycles of improvement are used, and only the last order within the convergence region is shown.

entropy does not change significantly at the accessible temperatures for either particle statistics as one dopes the system away from half filling. For $U = 8$ [Fig. 3(b)], the entropy for the fermionic system with 15% doping is larger than the half-filled value for $0.3 < T < 2$, while it does not change nearly as much with doping for 2HCBs for $T \gtrsim 0.9$. By increasing the interaction to $U = 16$, the agreement between the entropy of fermions and 2HCBs away from half filling improves, yet the deviations between the two for $n = 0.85$ start at much higher temperatures in comparison to the half filled case [see Fig. 3(c)]. These observations suggest that, even in the strong-coupling regime, the two systems away from half filling have fundamentally different phases.

Equation of state and compressibility

Further insight on the phases of the two systems at low temperatures can be gained by studying their equations of state and compressibilities. They are also of great interest to optical lattice experiments since those experiments are done in the presence of a confining potential that imposes a spatially varying chemical potential on the system. So, different regions in the trap correspond to different densities. In Fig. 4, we show n and $\partial n / \partial \mu$ vs μ at $T = 0.47$ for $U = 9$ and $U = 14$, which are below and above the critical interaction value for 2HCBs. From QMC calculations it is known that, for $U < U_c$, the ground state of 2HCBs does not have a charge density gap [16]. One can also infer from Fig. 4 that, regardless of the interaction strength, 2HCBs always have a smaller Mott gap at zero temperature than the fermions. This, in turn, implies that around half filling, the compressibility is always greater for bosons than for fermions, at any given temperature.

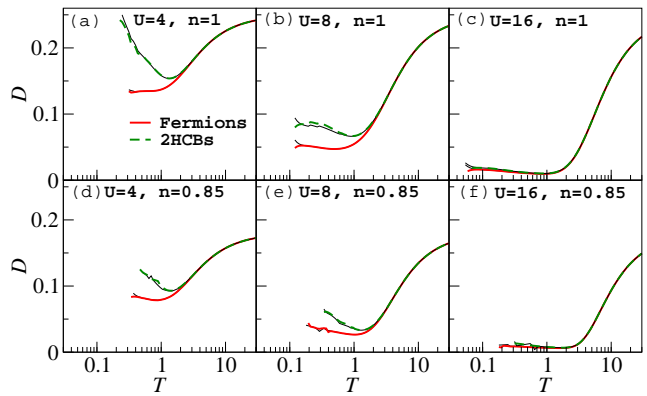


FIG. 5. (Color online) Double occupancy vs temperature for different values of U at half filling (top panels) and for $n = 0.85$ (bottom panels). In the weak-coupling regime with $U = 4$ [(a) and (d)], D for 2HCBs increases significantly by lowering the temperature below 1. Thick (color) lines are results from the last order and thin (black) lines are the results from the one-to-last order of the NLCEs after resummations.

Double occupancy

A slight upturn in the double occupancy (D) as one decreases T for the half-filled strongly-correlated fermionic system is a known phenomenon that has been attributed to the increase in virtual hoppings between allowed nearest neighbor sites due to the enhancement of short-range AF correlations [35]. In fact, the onset of this increase, which can be measured in the experiments, may serve as a universal probe for large AF correlations [36]. It can be shown to lead to adiabatic cooling by increasing the interaction strength [30], which is of great interest to optical lattice experiments. We have recently shown that such an increase in the double occupancy also occurs away from half-filling. Hence, in optical lattice experiments one also needs to make sure the density in most of the system is around half-filling in order for any increase in the double occupancy to be associated with the onset of antiferromagnetism [21].

We find interesting trends in the double occupancy of 2HCBs when compared to fermions, especially for weak interactions. As shown in Fig. 5, and unlike in the fermionic case, the double occupancy of 2HCBs at and away from half filling increases sharply below $T \sim 1$ for weak interactions, e.g., $U = 4$ in Figs. 5(a) and 5(d), while such a large difference between the results for the two particle statistics is absent for large U . The sharp low- T rise in D indicates that adiabatic cooling starting from the weakly interacting limit is efficient for 2HCBs [30]. The double occupancy for 2HCBs even reaches the uncorrelated value of $1/4$ in the half-filled case for $U = 4$ and $T \sim 0.2$, in stark contrast to D of the fermionic system. This is consistent with the absence of a Mott insulator for 2HCBs in that parameter region.

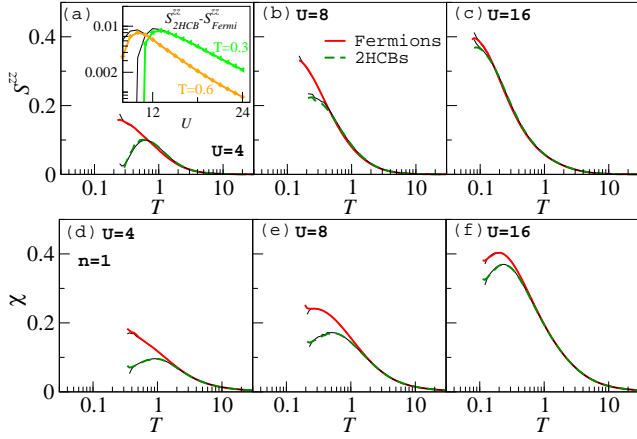


FIG. 6. (Color online) Nearest-neighbor spin correlations vs temperature at half filling for (a) $U = 4$, (b) $U = 8$, and (c) $U = 16$. (d)-(f) Uniform spin susceptibility at half filling vs temperature. Like for fermions, the spin susceptibility for 2HCBs peaks at a characteristic temperature T^* . The inset in (a) shows the exponential decrease of the difference between S^{zz} of 2HCBs and fermions at fixed temperatures by increasing U in the strong-coupling regime. Lines are the same as in Fig. 5

Spin correlations and uniform susceptibility

A related trend is also seen in the results for the NN spin correlations, $S^{zz} = |\langle \sum_{\delta} S_i^z S_{i+\delta}^z \rangle|$, where the sum runs over the four nearest neighbors of site i . As depicted in Fig. 6(a), S^{zz} for 2HCBs peaks around $T = 0.5$ when $U = 4$ before becoming vanishingly small at lower temperatures, which is again consistent with the superfluid nature of the ground state in this interaction region. On the other hand, it has been shown that for the fermionic case, S^{zz} at half filling grows monotonically by decreasing the temperature [32], which is consistent with its antiferromagnetically ordered low- T phase. It would be interesting to examine S^{zz} at $T = 0$ for 2HCBs and across the phase transition between the 2SF and the SCF phases, where S^{zz} is presumably not small. Here, the difference between results for fermions and 2HCBs sets in around $T = 1$ for $U = 4$ and, like all other thermodynamic quantities at half filling, becomes smaller as U is increased [see Figs. 6(a)-(c)]. As shown in the inset of Figs. 6(a), at fixed temperatures, this difference becomes exponentially small with increasing U in the strong-coupling regime.

Another thermodynamic quantity that highlights the difference between fermions and 2HCBs in the weak-coupling regime is the uniform spin susceptibility (χ). As seen in Fig. 6(d)-(f), we find that the deviation of χ for 2HCBs from that of fermions is large at low temperature for $U = 4$ and becomes smaller as U increases to 8 and 16. More importantly, whereas a previous QMC study by Paiva *et al.* [20] has shown that the peak location in the fermionic case changes non-monotonically by increasing U (following the variations of the AF cor-

relations in the system), for 2HCBs, the peak temperature decreases monotonically by increasing the interaction strength. This is because, unlike for fermions, the peak in χ for 2HCBs in the weak-coupling regime does not signify moment ordering, but rather the disappearance of well-defined moments. This can be understood from the fact that NN spin correlations also decrease around the same temperature [see Fig. 6(a)].

Attractive interactions

It is known for the fermionic Hubbard model that there exists the following unitary particle-hole transformation [37] that takes the repulsive Hubbard model to the attractive one:

$$\begin{aligned} \hat{f}_{j\uparrow} &= \hat{d}_{j\uparrow}, \\ \hat{f}_{j\downarrow} &= e^{i(\pi, \pi) \cdot \mathbf{R}_j} \hat{d}_{j\downarrow}^\dagger, \end{aligned} \quad (8)$$

where \mathbf{R}_j is the displacement vector of site j . To see the effect of the transformation more clearly, it is easier to rewrite the Hamiltonian of Eq. (1) in the so-called particle-hole symmetric form:

$$\begin{aligned} \hat{H} &= -t \sum_{\langle i,j \rangle \sigma} (\hat{f}_{i\sigma}^\dagger \hat{f}_{j\sigma} + \text{H.c.}) \\ &+ U \sum_i \left(\hat{n}_{i\uparrow} - \frac{1}{2} \right) \left(\hat{n}_{i\downarrow} - \frac{1}{2} \right) - \mu' \sum_i (\hat{n}_{i\uparrow} + \hat{n}_{i\downarrow}), \end{aligned} \quad (9)$$

where $\mu' = \mu - \frac{U}{2}$. The transformation in Eq. (8) leaves the hopping term, as well as $n_{i\uparrow}$, invariant, but changes $n_{i\downarrow}$ to $1 - n_{i\downarrow}$. As a result, the Hamiltonian in Eq. (9) is transformed to:

$$\begin{aligned} \hat{H} &= -t \sum_{\langle i,j \rangle \sigma} (\hat{d}_{i\sigma}^\dagger \hat{d}_{j\sigma} + \text{H.c.}) \\ &- U \sum_i \left(\hat{n}'_{i\uparrow} - \frac{1}{2} \right) \left(\hat{n}'_{i\downarrow} - \frac{1}{2} \right) - \mu' \sum_i (\hat{n}'_{i\uparrow} - \hat{n}'_{i\downarrow}) \end{aligned} \quad (10)$$

where $\hat{n}'_{i\sigma} = \hat{d}_{i\sigma}^\dagger \hat{d}_{i\sigma}$. At half filling ($\mu' = 0$), the only change from Eq. (9) will be the sign of the interaction U . Therefore, the energy spectral properties of the half-filled Fermi-Hubbard model, e.g., its specific heat, entropy, etc, are invariant under $U \rightarrow -U$. The nature of the ground state, however, is profoundly different in the repulsive and the attractive models since this transformation maps charge correlations to spin correlations and vice versa [38], which means that long-range AF order is mapped to a charge-density-wave one.

A similar unitary transformation maps the repulsive Hubbard model for 2HCBs to an attractive one:

$$\begin{aligned} \hat{b}_{j\uparrow} &= \hat{d}_{j\uparrow} \\ \hat{b}_{j\downarrow} &= \hat{d}_{j\downarrow}^\dagger. \end{aligned} \quad (11)$$

Therefore, similar to the fermionic case, the Hamiltonian is invariant under the change of sign of the interaction at

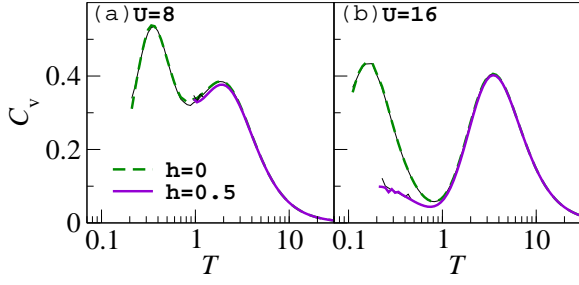


FIG. 7. (Color online) Specific heat of the repulsive Hubbard model for 2HCBs with and without a magnetic field, $h = 0.5$ and 0 , for (a) $U = 8$ and (b) $U = 16$. Thick (thin) lines are the results from the last (one-to-last) order of the NLCEs after numerical resummation.

half filling. The same argument presented above for the nature of the ground state of the fermionic model also applies to 2HCBs for $U > U_c$. In the regime $U < U_c$, we expect the 2SF phase to be the ground even with attractive interactions since, like the repulsive case, the system presumably gains more energy through the condensation of each specie than by minimizing the interaction energy.

As is clear from Eqs. (9) and (11), the attractive (repulsive) Hamiltonian away from half filling ($\mu' \neq 0$) is equivalent to the repulsive (attractive) one in the presence of a magnetic field in the z direction, h , a role that is played by the chemical potential in the attractive (repulsive) case. In Fig. 7, we show how the specific heat of the repulsive Hubbard model for 2HCBs is modified in the presence of such a field, by plotting C_v of the attractive model at $\mu' = 0$ and 0.5 ($h = 0$ and 0.5 for the repulsive case). The low temperature region is not accessible to us at small U and, in Fig. 7(a) for $U = 8$, only a small deviation around the high-temperature peak can be seen when the magnetic field is introduced. The results for $U = 16$ in Fig. 7(b) show a suppression of the specific heat at $T < 1$, which are consistent with the fact that spin degrees of freedom emerge only in the latter temperature region. Results for the fermionic case show qualitatively the same behavior as for 2HCBs for those two values of U .

Adiabatic cooling: implications for optical lattice experiments

Previously, we mapped out the isentropic paths of the 2D fermionic Hubbard model in the extended temperature-interaction space [21]. In Fig. 8(a), we present a similar diagram for 2HCBs. As expected from the large negative slope in the low- T double occupancy of 2HCBs for small U vs T (Fig. 5), adiabatic cooling by increasing U in the weak-coupling regime is much more efficient in comparison to the fermionic case. With the entropy per particle of 0.6 , T reduces roughly by a factor of 4 as the interaction increases from 1 to 24. However, the underlying physics in different regions of the diagram

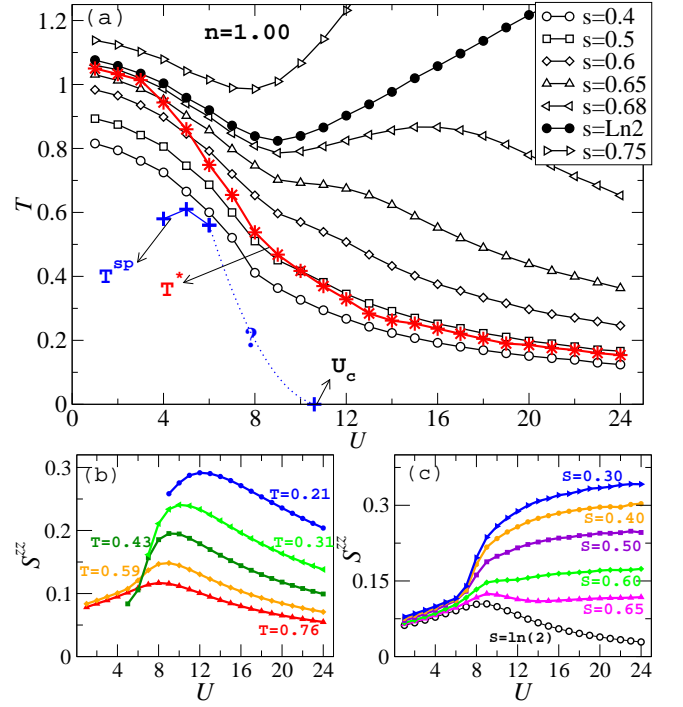


FIG. 8. (Color online) (a) Isentropic dependence of temperature on the interaction for different values of the entropy for the 2HCB-Hubbard model at half filling. Also shown in this panel is the characteristic temperature, T^* , which is the location of the peak in the uniform spin susceptibility, and T^{sp} , which is the location of the peak in the NN spin correlations. The exact values of the latter are at lower temperatures than what is accessible to us for $U < 4$ and $U > 6$. (b) Isothermic curves of S^{zz} vs U . (c) Isentropic curves of S^{zz} vs U for the entropy per particle from 0.3 to $\ln(2)$.

and the change in the strength of AF correlations is unlike that of fermions. As mentioned before, in the fermionic system, regardless of the value of the interaction, AF correlations are always enhanced by lowering the temperature. So, based on their dependence on U and how rapidly the temperature falls in the adiabatic cooling process, one could drive the fermionic system into the region with exponentially large AF correlations. The latter region could be identified by the onset of a downturn in the uniform susceptibility (T^*) [21].

On the contrary, for 2HCBs, the peak in the uniform susceptibility does not signify large AF correlations for weak interactions [see Figs. 6(a) and 6(d)]. We emphasize this by plotting in the same figure the location of the peak in S^{zz} (T^{sp}) for a few values of U . Beyond U_c , where the Mott insulating ground state not only has long-range xy -ferromagnetic order, but also very large z -antiferromagnetic correlations, the maximum of S^{zz} is likely at zero temperature.

Results in Fig. 8(b) and Fig. 8(c) provide further insight into the behavior of S^{zz} for different interaction strengths. By comparing these figures to their fermionic counterparts [Figs. 3(c) and 3(d) in Ref. 21], one can see

that unlike in the weak-coupling regime, where the results are qualitatively different for the two particle statistics, in the strong-coupling regime they are very similar [as shown in Fig. 6(a), the difference decreases exponentially with U]. As seen in Fig. 8(b), at fixed (and low) temperatures S^{zz} for 2HCBs sharply drops to small values by decreasing U . In Fig. 8(c), the isentropic curves of S^{zz} are almost on top of each other for $U \lesssim 7$ for the entropies shown, and are expected to become vanishingly small at lower entropies that are not accessible to us. This is, again, unlike the trends in the fermionic model in the weak-coupling regime. The opposite is true, however, for $U > U_c$ where, at the entropies accessible to us, S^{zz} values of 2HCBs agree very well with their fermionic counterparts.

So far, much lower temperatures have been achieved with bosons in optical lattices than with fermions. Employing novel cooling techniques, researchers have been able to access temperatures as low as 1 nK with bosons deep in the Mott insulating regime [39]. It has also been shown in experiments with bosonic mixtures and that the inter- and intra-specie interactions can be tuned using Feshbach resonance and other techniques [7, 9, 10]. Our results show that thermodynamic properties and short-range AF correlations of 2HCBs are very (exponentially) close to those of the fermions for strong interactions and up to intermediate to low temperatures. Therefore, by engineering the strong interaction regime studied here, optical lattice experiments with two-component bosons could also provide a tool for simulating intermediate to low temperature correlations in the Fermi-Hubbard model. Further studies need to be done to explore the properties of 2HCBs away from half filling and examine their relevance to the fermionic case.

IV. CONCLUSIONS

We have examined the particle statistics dependence of the thermodynamic properties of the 2D Hubbard model by means of an exact method (NLCEs) that yields properties such as entropy, specific heat, double occupancy, and spin correlations in the thermodynamic limit. The results are valid above a certain temperature that depends on the interaction and the filling factor. We considered two-component fermions and 2HCBs and compared their properties at various temperatures and interaction strengths, up to three times the bandwidth.

We have shown that for weak interactions, in the regime where the ground state of the two models at half filling have fundamentally different natures, the results for observables at finite temperature differ significantly for the two particle statistics starting at relatively high temperatures. In contrast, in the strong-coupling regime (beyond a critical interaction that separates a superfluid from a Mott insulator phase for 2HCBs), the agreement between the thermodynamic quantities of the two systems, including short-range AF correlations, extends to much lower temperatures. We find that the trends in spin correlations in the z direction are similar for both particle statistics and that the results differ only by exponentially small values for strong interactions. This provides an additional tool to probe correlations of fermionic systems in optical lattice experiments by emulating them using two-specie bosons, which can generally be cooled down to lower temperatures.

ACKNOWLEDGMENTS

This work was supported by the NSF under Grant No. OCI-0904597. We thank J. Carrasquilla for useful discussions.

-
- [1] P. W. Anderson, *Science* **235**, 1196 (1987).
 - [2] For a review, see E. Dagotto, *Rev. Mod. Phys.* **66**, 763 (1994).
 - [3] D. Jaksch, C. Bruder, J. I. Cirac, C. W. Gardiner, and P. Zoller, *Phys. Rev. Lett.* **81**, 3108 (1998).
 - [4] M. Greiner, O. Mandel, T. Esslinger, T. Hansch, and I. Bloch, *Nature (London)* **415**, 39 (2002); K. Jiménez-García, R. L. Compton, Y. -J. Lin, W. D. Phillips, J. V. Porto, and I. B. Spielman, *Phys. Rev. Lett.* **105**, 110401 (2010).
 - [5] R. Jordens, N. Strohmaier, K. Gunter, H. Moritz, and T. Esslinger, *Nature (London)* **455**, 204 (2008); U. Schneider, L. Hackermüller, S. Will, Th. Best, I. Bloch, T. A. Costi, R. W. Helmes, D. Rasch, A. Rosch, *Science* **322**, 1520 (2008).
 - [6] I. Bloch, J. Dalibard, and W. Zwerger, *Rev. Mod. Phys.* **80**, 885 (2008).
 - [7] G. Thalhammer, G. Barontini, L. De Sarlo, J. Catani, F. Minardi, and M. Inguscio, *Phys. Rev. Lett.* **100**, 210402 (2008).
 - [8] S. Trotzky, P. Cheinet, S. Fölling, M. Feld, U. Schnorrberger, A. M. Rey, A. Polkovnikov, E. A. Demler, M. D. Lukin, and I. Bloch, *Science* **319**, 295 (2008).
 - [9] B. Gadway, D. Pertot, R. Reimann, and D. Schneble, *Phys. Rev. Lett.* **105**, 045303 (2010).
 - [10] J. Simon, W. S. Bakr, R. Ma, M. E. Tai, P. M. Preiss, and M. Greiner, *Nature (London)* **472**, 307 (2011).
 - [11] E. Altman, W. Hofstetter, E. Demler, and M. D. Lukin, *New Journal of Physics* **5**, 113 (2003).
 - [12] L.-M. Duan, E. Demler, and M. D. Lukin, *Phys. Rev. Lett.* **91**, 090402 (2003).
 - [13] A. B. Kuklov and B. V. Svistunov, *Phys. Rev. Lett.* **90**, 100401 (2003).
 - [14] A. Isacsson, M.-C. Cha, K. Sengupta, and S. M. Girvin, *Phys. Rev. B* **72**, 184507 (2005).

- [15] A. Hubener, M. Snoek, and W. Hofstetter, *Phys. Rev. B* **80**, 245109 (2009).
- [16] Ş. G. Söyler, B. Capogrosso-Sansone, N. V. Prokof'ev, and B. V. Svistunov, *New Journal of Physics* **11**, 073036 (2009).
- [17] B. Capogrosso-Sansone, Ş. G. Söyler, N. V. Prokof'ev, and B. V. Svistunov, *Phys. Rev. A* **81**, 053622 (2010).
- [18] M. Boninsegni, *Phys. Rev. Lett.* **87**, 087201 (2001).
- [19] Y. Nakano, T. Ishima, N. Kobayashi, K. Sakakibara, I. Ichinose, and T. Matsui, *Phys. Rev. B* **83**, 235116 (2011); Y. Nakano, T. Ishima, N. Kobayashi, T. Yamamoto, I. Ichinose, and T. Matsui, *Phys. Rev. A* **85**, 023617 (2012).
- [20] T. Paiva, R. Scalettar, M. Randeria, and N. Trivedi, *Phys. Rev. Lett.* **104**, 066406 (2010); S. Chiesa, C. N. Varney, M. Rigol, and R. T. Scalettar, *Phys. Rev. Lett.* **106**, 035301 (2011); T. Paiva, Y. L. Loh, M. Randeria, R. T. Scalettar, and N. Trivedi, *Phys. Rev. Lett.* **107**, 086401 (2011); S. Fuchs, E. Gull, L. Pollet, E. Burovski, E. Kozik, T. Pruschke, and M. Troyer, *Phys. Rev. Lett.* **106**, 030401 (2011).
- [21] E. Khatami and M. Rigol, *Phys. Rev. A* **84**, 053611 (2011).
- [22] S. Chen, J. Cao, and S.-J. Gu, *Europhys. Lett.* **85**, 60004 (2009).
- [23] X. Dai, M. Ma, and F.-C. Zhang, *Phys. Rev. B* **72**, 132504 (2005).
- [24] S. Guertler, M. Troyer, and F.-C. Zhang, *Phys. Rev. B* **77**, 184505 (2008).
- [25] Y. Li, M. R. Bakhtiari, L. He, and W. Hofstetter, *Phys. Rev. A* **85**, 023624 (2012).
- [26] T. Ohgoe and N. Kawashima, *Phys. Rev. A* **83**, 023622 (2011).
- [27] S. Powell, *Phys. Rev. A* **79**, 053614 (2009).
- [28] M. Rigol, T. Bryant, and R. R. P. Singh, *Phys. Rev. Lett.* **97**, 187202 (2006); *Phys. Rev. E* **75**, 061118 (2007).
- [29] M. Rigol, T. Bryant, and R. R. P. Singh, *Phys. Rev. E* **75**, 061119 (2007).
- [30] F. Werner, O. Parcollet, A. Georges, and S. R. Hassan, *Phys. Rev. Lett.* **95**, 056401 (2005).
- [31] K. Mielsonson, E. Khatami, D. Galanakis, A. Macridin, J. Moreno, and M. Jarrell, *Phys. Rev. B* **80**, 140505 (2009).
- [32] T. Paiva, R. T. Scalettar, C. Huscroft, and A. K. McMah-an, *Phys. Rev. B* **63**, 125116 (2001).
- [33] D. Duffy and A. Moreo, *Phys. Rev. B* **55**, 12918 (1997).
- [34] D. Vollhardt, *Phys. Rev. Lett.* **78**, 1307 (1997).
- [35] E. V. Gorelik, I. Titvinidze, W. Hofstetter, M. Snoek, and N. Blümer, *Phys. Rev. Lett.* **105**, 065301 (2010).
- [36] E. V. Gorelik, D. Rost, T. Paiva, R. Scalettar, A. Klümper, and N. Blümer, *Phys. Rev. A* **85**, 061602(R) (2012).
- [37] H. Shiba, *Progress of Theoretical Physics* **48**, 2171 (1972).
- [38] J. E. Hirsch, *Phys. Rev. B* **31**, 4403 (1985).
- [39] D. M. Weld, P. Medley, H. Miyake, D. Hucul, D. E. Pritchard, and W. Ketterle, *Phys. Rev. Lett.* **103**, 245301 (2009).